

# Multi-Channel Scanning Filter Spectrometer for the Beam Emission Spectroscopy

Viktoriia OLEVSKAIA, Tatsuya KOBAYASHI<sup>1)</sup>, Katsumi IDA<sup>1)</sup>,  
Mikirou YOSHINUMA<sup>1)</sup> and Wenqing HU<sup>2)</sup>

*Max Plank Institute for Plasma Physics, Garching 85748, Germany*

*Physik-Department E28, Technical University Munich, Garching 85748, Germany*

<sup>1)</sup>*National Institute for Fusion Science, Toki, Gifu 509-5292, Japan*

<sup>2)</sup>*Iwate University, Faculty of Science and Engineering, Morioka, Iwate 020-8551, Japan*

(Received 7 November 2018 / Accepted 20 May 2019)

Multi-channel scanning filter spectrometer with narrow band pass of 2 nm is installed in Large Helical Device (LHD) for Beam Emission Spectroscopy (BES) using hydrogen (H) and deuterium beam (D). The spectral shape of transmitted light (half width at half maximum, skewness and kurtosis) is measured using the monitor grating spectrometer coupled with the filter spectrometer. No distortion of the spectrum shape is observed in the wavelength scan range of 8 nm required for the Doppler shift of the BES emission from H-beam and D-beam.

© 2019 The Japan Society of Plasma Science and Nuclear Fusion Research

Keywords: BES, multi-channel filter spectrometer, LHD

DOI: 10.1585/pfr.14.1305118

Beam Emission Spectroscopy (BES) is a diagnostic system for local plasma density measurement and is widely used in fusion devices, such as DIII-D [1], LHD [2, 3], KSTAR [4] and MAST [5]. In the case of the BES system in LHD, Neutral Beam Injection (NBI) heating emits light from the collisionally excited neutral beam atoms, which is collected by optical fibers. Fibers lead light to spectroscopic devices for distinguishing beam emission components from background emission components and then to detectors. Since the beam injection direction and the lines of sight for the BES are not set to be perfectly orthogonal, the beam emission components have a finite Doppler shift from  $H_\alpha$  line, which is measured. Due to non-axisymmetric field configuration of the magnetic field, it is challenging to use BES systems in helical devices. Even with such difficulty, BES systems were implemented in the Compact Helical Device (CHS) [6] and later in the Heliotron J [7] successfully.

In LHD, NBI can use different species (Hydrogen or Deuterium beam) to produce plasmas having high purity hydrogen or deuterium content, which is a very important feature for studying the isotope effect on turbulence and transport. To cover the Doppler shift from H-beam and D-beam, the system must have a wide scanning range of transmitted wavelength. Conventional BES lacks the capability to scan the wavelength range, which is large enough. Previously, a grating spectrometer was used for a BES system that has a wide range of the wavelength scan [8]. Recently, to increase the spatial resolution and number of channels together with keeping a wide scanning range, the

new BES system with filter tilting and 256 fibers has been developed. An advantage of the new BES in LHD is the narrow bandwidth of 2 nm. This bandwidth is necessary to eliminate the interference of impurity and passive  $H_\alpha$  light. Furthermore, the presented multi-channel system is rather compact. Only one filter with a large enough diameter is used for filtering all signals in 64 channels.

To realize such a system, it is necessary to examine the characteristics of transmitted spectrum and the capacity of control wavelength change. The article presents a description of the new BES system and a characterization of the filter system.

At the left side of the setup, light comes from an array of optical fibers ( $16 \times 16$ ) and travels to the large diameter ( $\phi = 160$  mm) high dispersion filter, as shown in Fig. 1 (top). Filter allows only a certain wavelength to pass. The thickness of the filter is 4 mm. Optical path shifts in parallel between two lenses. However, the image on the detector does not shift because the image is produced by the lens. With rotation of the filter the passing wavelength can be changed, thus the range of wavelengths can be covered. After filtering, light travels to the Avalanche Photodiode camera (APDCAM provided by Fusion Instruments Kft., Budapest, Hungary) for detection. The reason for using APDCAM instead of a common CCD camera is the higher sampling rate (1 MHz over 1 kHz for CCD). Such a high sampling is necessary to detect rapid fluctuations. The front view of APDCAM detector is presented in Fig. 1 (bottom). Detector has  $8 \times 8$  elements and 64 channels in total. The shape of the detector is square, with the length of 1.6 mm. The diameter of the input fiber is

author's e-mail: volev@ipp.mpg.de

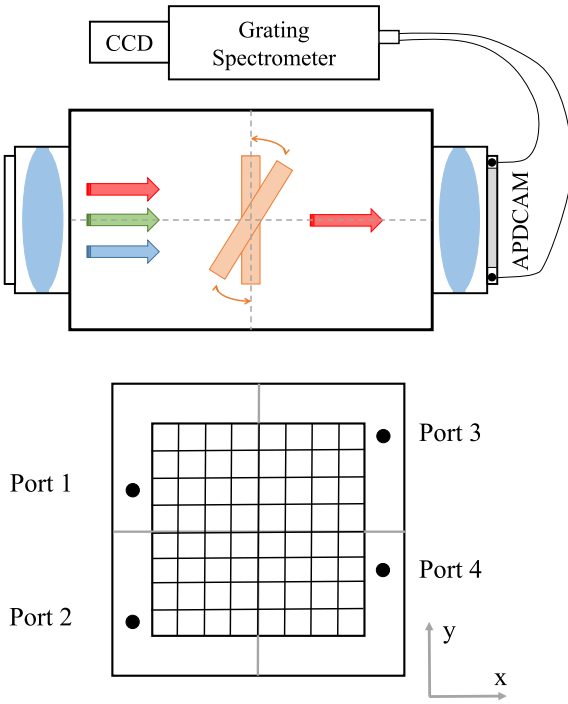


Fig. 1 Setup of BES analyzing part (top) and front view of APDCAM detector (bottom).

0.8 mm, and in one detector four spots of the optical fibers are set. Therefore, light from four optical fibers goes to one detector cell. Also, APDCAM detector panel has 4 additional ports with optical fibers which lead the light to the ordinary grating spectrometer for a quick check of the transmitted spectrum. These additional ports 1-4 were used for investigation of filter properties and its characterization.

As mentioned above, Doppler shifted  $H_\alpha$  line is measured in BES diagnostics. The filter is used for distinguishing the line from background emission. In LHD, the beam species of the NBI can be changed. Therefore, the spectrometer should have the capacity of wavelength change. By rotation of the filter we can scan through a range of wavelengths, thus the filter is used as a spectroscopic device.

To utilize this idea, the transmitted spectrum must remain unchanged when the filter angle is changed. In order to examine this point, we performed a bench test by using white Halogen light source. The signal was recorded by CCD camera through optical fibers in ports 1-4. As an example, data for port 1 is shown in Fig. 2 (a). Signal was normalized on its maximum. It can be seen that by changing of the rotation angle (from  $-15^\circ$  to  $0^\circ$ ) one can change the central wavelength. Rotation was performed from position perpendicular to the optical axis ( $0^\circ$ ) to the counter-clockwise direction (that is why the sign is negative). Of course, rotation in clockwise direction is also possible.

It is important to know how properties of the line shape are changed with the rotation of the filter. As was

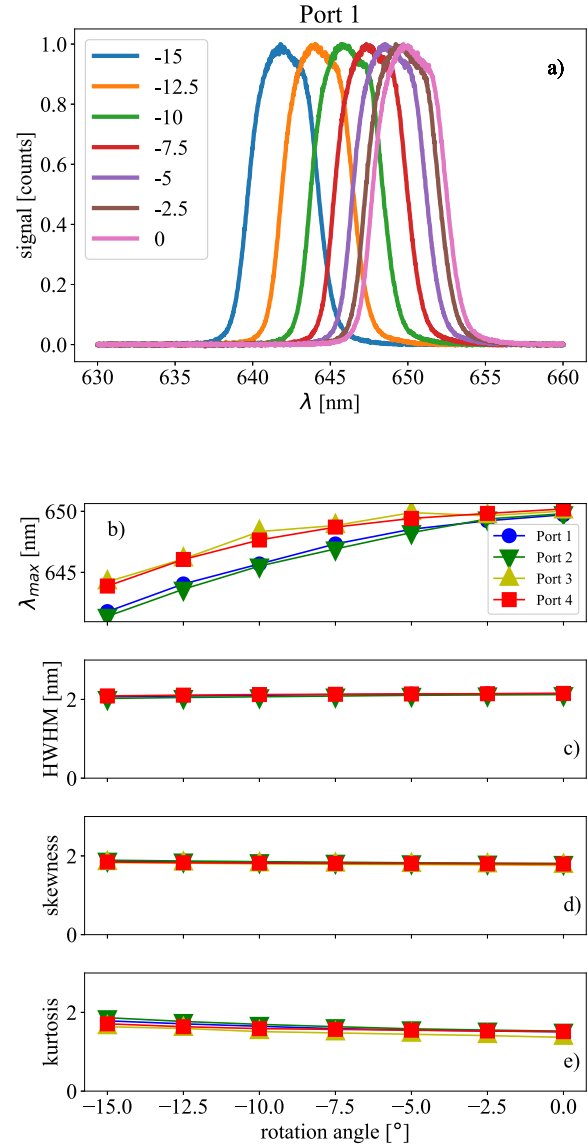


Fig. 2 Normalized data for port 1 (a) and characteristics of line-shape (b-e).

shown above for the port 1, central wavelength is changed. That is also the case for all the ports. See Fig. 2 (b). Other properties of spectrum shape (half width on half maximum (HWHM), skewness, and kurtosis) for all the signals from all the ports are almost the same. See Figs. 2 (c-e). This means that the rotation of the filter does not influence the shape of the signal. More quantitatively, the change in the HWHM is less than 5% during this experiment. Similarly, changes in skewness and kurtosis are less than 5% and 15%, respectively.

Difference in kurtosis seems to be noticeable, up to 15%. However, since kurtosis is the fourth order moment, it is only sensitive to the small differences away from peak. As can be seen in Fig. 3, for the spectra with the largest ( $-15^\circ$ ) and the smallest ( $0^\circ$ ) kurtosis in Port 2, bulk part of the spectra is approximately the same. Hence, this change can be neglected for our purpose.

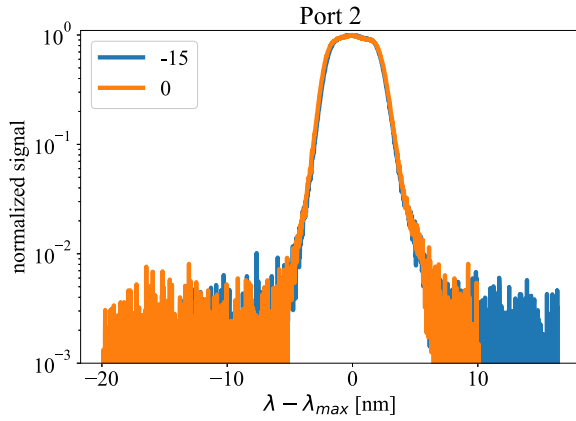


Fig. 3 Two different spectra that have the largest and the smallest kurtosis, normalized by the peak value and offset by the wavelength of the peak.

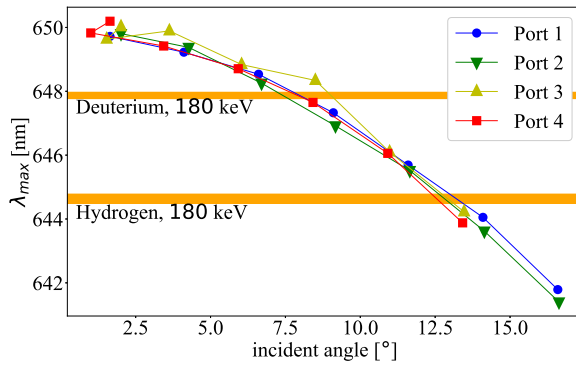


Fig. 4 Wavelength dependence on incident angle. Range of necessary wavelengths is highlighted.

Central wavelength dependence has different offsets for different ports. This is due to different location of the ports from the center of the detector. It is better to consider incident angle of light given by Eq. (1).

$$\gamma = \cos^{-1} \left( \frac{f \cos \theta - x \sin \theta}{\sqrt{x^2 + y^2 + f^2}} \right), \quad (1)$$

where  $f$  is focal length,  $\theta$  is rotation angle, and  $x, y$  are coordinates of fiber ports.

The central wavelength was plotted as a function of the incident angle in Fig. 4. All the points are aligned in a single curve with a finite level of deviation, which is due to noise contribution. The central wavelength is predicted to behave as the formula:

$$\lambda^2 = \lambda_0^2 \left( 1 - \left( \frac{N_e}{N^*} \right)^2 \sin^2 \gamma \right), \quad (2)$$

where  $\gamma$  is incident angle,  $N_e \sim 1$  is dispersion index for air,  $N^*$  is dispersion angle for the filter, and  $\lambda_0$  is central wavelength when  $\gamma = 0$ , which is designed by choosing proper values of the filter thickness  $d$  and the filter dispersion index  $N^*$ . The curve from Fig. 4 was fitted, and parameters  $N^*$  and  $\lambda_0$  were found as  $1.8 \pm 0.2$  and

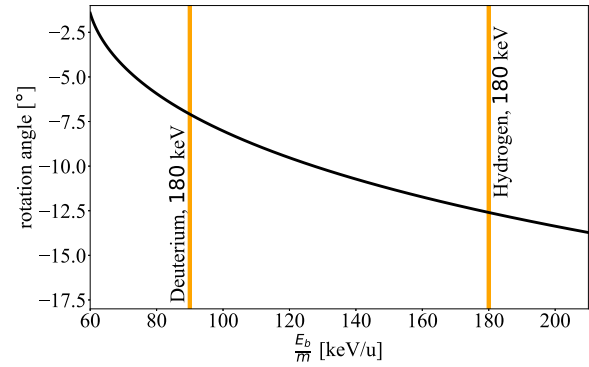


Fig. 5 Rotation angle dependence on energy-mass ratio of the injected beam. Range of needed energy-mass ratio is highlighted.

$649.7 \pm 0.1$  nm, respectively.

The wavelength of the expected Doppler shift in LHD at the beam axis is:

- Deuterium, 180 keV: 647.77 – 647.97 nm
- Hydrogen, 180 keV: 644.49 – 644.78 nm

From Fig. 4 one can see that this range is covered. A finite range of expected wavelength is due to different angles between the lines of sight and the beam direction.

In the presented paper the spectroscopic properties of multi-channel filter spectrometer for BES system in LHD was shown. Rotating filter is proven to be a good spectroscopic scheme to change the transmitted wavelength. First, the rotating filter covers a wide range of wavelengths (8 nm), including those that we are interested in (Hydrogen and Deuterium Doppler shift). Second, this filter system has a negligible effect on line shape of signal.

At the center of the APD cell ( $x = y = 0$ ) the incident angle  $\gamma$  is equal to the rotation angle  $\theta$ . Thus, we can derive dependence of rotation angle on the wavelength as shown at Eq. (3). This formula allows to determine the necessary tilt angle of the filter for the target central wavelength to be observed, that corresponds to the beam energy of NBI.

$$\theta \sim \sin \theta = \frac{N^*}{N_e} \sqrt{1 - \left( \frac{\lambda}{\lambda_0} \right)^2}. \quad (3)$$

Wavelength of Doppler shifted line is defined as:

$$\lambda = \lambda_\alpha + \lambda_\alpha \frac{V_b}{c} \cos \phi = \lambda_\alpha + \lambda_\alpha \frac{\sqrt{2E_b/m}}{c} \cos \phi, \quad (4)$$

where  $\lambda_\alpha = 656.2$  nm is  $H_\alpha/D_\alpha$  line,  $V_b$  is beam velocity,  $E_b$  is beam energy,  $m$  is mass of species,  $c$  is speed of light and  $\phi = 150^\circ$  is angle between lines of sight and beam injection direction.

To treat both Deuterium and Hydrogen beams, from Eqs. (3) and (4) one can derive dependence of the tilt angle on the beam energy, as shown in Eq. (5). Figure 5 represents this formula and it can be seen that for Deu-

terium beam rotation angle  $\theta = -7^\circ$  and for Hydrogen beam  $\theta = -12.5^\circ$  is needed.

$$\theta = \frac{N^*}{N_e} \sqrt{1 - \left(\frac{\lambda_\alpha}{\lambda_0}\right)^2 \left(1 + \frac{\cos \phi}{c} \sqrt{\frac{2E_b}{m}}\right)^2}. \quad (5)$$

This work is partly supported by the National Institute for Fusion Science grant administrative budget (ULHH033) and the Grant-in-Aid for Scientific Research of JSPS (15H02336). The authors would also like to thank Gregor Birkenmeier, Max Plank Institute for Plasma

Physics (Garching, Germany), for strong support and useful discussion.

- [1] G.R. McKee *et al.*, Rev. Sci. Instrum. **74**, 2014 (2003).
- [2] T. Oishi *et al.*, Rev. Sci. Instrum. **81**, 10D719 (2010).
- [3] M. Ono *et al.*, Plasma Fusion Res. **11**, 1402115 (2016).
- [4] Y.U. Nam *et al.*, Rev. Sci. Instrum. **83**, 10D531 (2012).
- [5] A.R. Field *et al.*, Rev. Sci. Instrum. **83**, 013508 (2012).
- [6] T. Oishi *et al.*, Nucl. Fusion **46**, 317 (2006).
- [7] S. Kobayashi *et al.*, Rev. Sci. Instrum. **83**, 10D535 (2012).
- [8] S. Kado *et al.*, Rev. Sci. Instrum. **81**, 10D720 (2010).